TITLE: Quantifying the link between crop production and mined groundwater irrigation in China

AUTHORS:

Danielle S. Grogan[1*], Fan Zhang[2], Alexander Prusevich[1], Richard B. Lammers[1], Dominik Wisser[1,3], Stanley Glidden[1], Changsheng Li[1], Steve Frolking[1]

[1]Institute for the Study of Earth, Oceans, and Space, University of New Hampshire, Durham, NH, USA

[2]Department of Environmental Science and Technology, School of Human Settlement and Civil Engineering, Xi'an Jiaotong University, Xi'an China

[3]Center for Development Research, University of Bonn, Bonn, Germany

*Corresponding author. Address: Earth Systems Research Center, Water Systems Analysis Group, University of New Hampshire. 8 College Road, Durham, NH 03820.

email address: Danielle.grogan@wildcats.unh.edu

ABSTRACT

In response to increasing demand for food, Chinese agriculture has both expanded and intensified over the past several decades. Irrigation has played a key role in increasing crop production, and groundwater is now an important source of irrigation water. Groundwater abstraction in excess of recharge (i.e., groundwater mining) has resulted in declining groundwater levels and could eventually restrict groundwater availability. In this study we used a hydrological model, WBMplus, in conjunction with a process based crop growth model, DNDC, to evaluate Chinese agriculture's recent dependence upon mined groundwater, and to quantify mined groundwater-dependent crop production across a domain that includes variation in climate, crop choice, and management practices. This methodology allowed for the direct attribution of crop production to irrigation water from rivers and reservoirs, shallow (renewable) groundwater, and mined groundwater. Simulating 20 years of weather variability and circa year 2000 crop areas, we found that mined groundwater fulfilled 20% - 49% of gross irrigation water demand, assuming all demand was met. Mined groundwater accounted for 15% - 27% of national total crop production. There was high spatial variability across China in irrigation water demand and crop production derived from mined groundwater. We find that climate variability and mined groundwater demand do not operate independently, but rather magnify one another in hot and dry years with increased irrigation demand and limited surface water supply for irrigation.

1. INTRODUCTION

Increasing global demand for food over the past several decades has forced agriculture to expand into water-scarce regions and increase irrigation water use substantially [*Molden et al*., 2007].

With little additional land available for agricultural expansion except in tropical rainforests, future increases in crop production will likely rely on increases in irrigation and intensification, both in China and globally [*Molden et a.,* 2007]. Historically, China's agriculture was concentrated in the wetter southern half of the country, but significant expansion over the past 50 years has led to over 50% of current national crop production occurring in the dry northern regions [*Ma,* 2006]. Irrigated agriculture has expanded significantly in China in the past 75 years, increasing by more than 35 million hectares since 1939 to 51 Mha of planted land and 79 Mha of harvested land in 2000 [*Calow et al*., 2009; *Portmann et al.,* 2010]. Groundwater exploitation has underpinned the agricultural intensification of northern China since the 1990's, where groundwater accounts for up to 40% of irrigation water [*Wada et al.* 2012]. Declining groundwater levels are threatening to limit the irrigation water supply for China's crop production [*Kang et al.,* 2009; *Aeschbach-Hertig and Gleeson*, 2012*; Syed et al.,* 2008]. There has been a 15 m drop in groundwater levels in the North China Plain since 1960 [*Calow et al.,* 2009], and the current rate of groundwater depletion across China is approximately 1m per year [*Aeschbach-Hertig and Gleeson*, 2012]. This heavy reliance on groundwater for irrigation is driven largely by lack of sufficient surface water supplies [*Wisser et al.,* 2008; *Wada et al.,* 2012], and Northern China is now considered to be a region of physical water scarcity, i.e., more than 75% of river discharge is abstracted [*Molden et al*., 2007]. Global multi-model projections of irrigation water availability show significant reduction in Northern China for irrigation potential from renewable surface water by 2100 due to climate change (using a scenario of high greenhouse gas emissions (RCP8.5) [*Elliott et al*., 2013]. Aquifer depletion could also significantly decrease irrigation water availability in the future. Despite the importance of groundwater and groundwater depletion for the future of Chinese agriculture, it is currently

unknown how much food is produced as a direct result of irrigation with non-renewable groundwater mining.

Large-scale surface water balance models can simulate the use of both surface water and groundwater for irrigation. Several model-based estimates of irrigation water demand in China have been made, ranging from 220 to 850 $km^3\ yr^{-1}$, circa 2000 [*Wisser et al*., 2008], with most estimates in the range of 350 – 500 $km^3\ yr^{-1}$ [*Döll and Siebert,* 2002; *Siebert and Döll,* 2007; *Liu and Yang,* 2010; *Wada et al.,* 2012]. The proportion of irrigation water demand fulfilled by mined groundwater pumping is less well constrained. Groundwater (both renewable and mined in excess of recharge) provides up to 40% of China's irrigation water, and model results from Wada et al. [2012] show that 20 $km^3\ yr^{-1}$ (5% of irrigation demand) is drawn from non-renewable groundwater.

Water supply alone does not determine food production; cropped areas, crop choice, soil quality, and management practices all contribute [*Tilman et al*., 2002; *Foley et al*., 2012]. Agriculture's vulnerability to changes in water supply will necessarily also depend on these factors, which all vary spatially across China. Crop water productivity, the crop yield gained from one unit of water, also varies spatially, even within individual watersheds [*Cai et al.,* 2011]. Global-scale studies of unsustainable water supplies and food production have used an empirical method to determine the relationship between water use and crop yields [*Siebert and Döll*, 2010], but this method is not suited for higher-resolution analysis [*Siebert and Döll*, 2010]. An alternative approach is to employ a process-based crop growth model that can capture these important spatially-variable production factors [*Müller et al*, 2013].

In this study, we used a hydrological model in conjunction with a process based crop growth model to evaluate Chinese agriculture's dependence upon mined groundwater, and quantify mined groundwater-dependent crop production across a domain that includes variation in climate, crop choice, and management practices. We computed irrigation water demand, as well as sources of water supply, across 20 years of climate variability. Using these two models allowed us to quantify the amount of food produced as a direct result of irrigation with groundwater mined in excess of recharge. We also defined an index of vulnerability to loss of mined groundwater resources that is a function of the amount of mined groundwater required for irrigation and the productivity of a crop irrigated from that water source.

2. METHODS

We used two models to simulate irrigation water demand, irrigated and rainfed crop yields, and crop production due to mined groundwater. A grid-based water balance model [WBMplus, *Wisser et al*., 2010] calculated daily fluxes and storage of water between and within different water storage pools (Figure 1). WBMplus was used to estimate the irrigation water demand of different crop types based on weather variables, soil properties, and crop parameters, and tracked the sources of irrigation water available to meet that demand [e.g., *Wisser et al.,* 2008]. DNDC [*Li et al.,* 1992; 2007], a process-based crop growth and agroecosystem biogeochemistry model, was used to simulate fully-irrigated and rainfed crop yields for individual crops and multi-cropping systems for all counties in China. WBMplus provided an estimate of the irrigated crop area dependent upon mined groundwater. By applying DNDC's difference between irrigated crop yields and rainfed crop yields to these areas, we estimated the portion of total crop yields

directly resulting from groundwater mining.

2.1 Water Balance Model

WBMplus computed a daily water balance for each 0.5 degree grid cell. Water was input through precipitation and irrigation, and outputs were evapotranspiration, runoff, and shallow rechargeable groundwater (Figure 1). Water was stored as soil moisture and in the shallow groundwater pool. Surface runoff and baseflow from shallow groundwater were transported downstream through the STN-30p river network [*Vorosmarty et al*., 2000] taking into account the storage of water in large reservoirs. A detailed description of WBMplus's fundamental processes is given by Wisser et al. [2010]. Here we describe WBMplus's method of irrigation and crop water use (Section 2.1.1), and WBMplus's updated method of simulating operation of large reservoirs (Section 2.1.2).

2.1.1 Irrigation and crop ET

Irrigation was simulated by abstracting water from rivers, reservoirs, and groundwater, then moving that water to the soil water pool. The amount of water abstracted was determined by an irrigation water demand that was based on root zone soil moisture, crop evapotranspiration, and irrigation efficiency. Evapotranspiration depended on each crop's planting date, growing season length, growth stages, rooting depth, and a crop water use coefficient. Crop coefficients, growth stages, rooting depths, and depletion factors were from Siebert and Döll [2010], and the coefficient method used was based on FAO recommendations [*Allen*, 1998]. Each crop's evapotranspiration was calculated as:

$$E_c = K_c ET_0 \qquad (1)$$

Where E_c [mm day^{-1}] is the crop's evapotranspiration, Kc [-] is a dimensionless crop- dependent and growth stage-dependent coefficient for crop c, and ET_0 [mm day^{-1}] is a reference-surface potential evapotranspiration. ET_0 was calculated using the Hamon method [*Hamon,* 1963; *Vorosmarty et al.,* 1998].

Crop evapotranspiration and percolation removed water from the soil moisture pool. When water inputs to the soil moisture pool brought the soil moisture stock above field capacity, the excess was diverted in equal proportions to surface runoff and percolation. Percolated water moved to the shallow groundwater storage pool (implemented as a linear reservoir); water from the groundwater storage pool flowed to the river network as baseflow. A daily soil moisture accounting was done in irrigated areas with inputs from precipitation, irrigation water, and snowmelt, and with evapotranspiration and percolation as outputs from the soil storage. If soil moisture fell below a crop-dependent threshold, C_t [mm], irrigation water was applied to bring the soil moisture up to field capacity. The crop-dependent threshold for soil moisture was calculated as:

$$C_t = C_s * R_d(F_{cap} - W_{pt}) \quad (2)$$

Where C_s [-] is a crop-specific scalar that represents a crop's inability to remove all water from the soil, R_d [mm] is the crop's rooting depth, F_{cap} [-] is the field capacity of the soil, and W_{pt} [-] is the wilting point of the soil. Crop-specific parameters C_s and R_d were from Siebert and Döll [2010], and F_{cap} and W_{pt} are from FAO/UNESCO [2003].

When soil moisture was below the crop-specific threshold, the crop had a positive irrigation demand (otherwise demand was zero). For each grid cell, a net irrigation demand, I_{net} [mm day^{-1}], was calculated daily as the area-weighted water demand of all the crops [26 crop types; taken from *Portmann et al*., 2010] in the grid cell. Daily net irrigation demand was calculated as:

$$I_{net} = \sum_{c=1}^{n} A_i \cdot a_i \cdot \mathrm{I}_c \quad (3)$$

where A_I [-] is the portion of the grid cell's area equipped for irrigation, a_c [-] is the portion of the irrigated area containing crop c (Table 1), I_c [mm day^{-1}] is the irrigation demand of crop c, and n is the number of crops.

Rice paddies require additional irrigation water due to inundation-induced percolation. We assumed that irrigation water was applied to rice paddies to maintain a 50 mm flooding depth throughout the growing season. To achieve this, irrigation water was applied on the first day of the paddy rice-growing season to fill the soil moisture pool 50 mm above field capacity, and each subsequent day water was applied to account for percolation plus evapotranspiration losses minus precipitation gains. Rice paddy percolation was assumed to occur at a constant rate that is determined by the soil drainage class [e.g., *Wisser et al*., 2008], estimated spatially from the FAO/UNESCO soil map of the world [*FAO/UNESCO,* 2002].

In each grid cell, water for irrigation could be withdrawn from large reservoir storage (see §2.1.2 below), if present, rivers flowing through the grid cell, shallow renewable groundwater, and

mined groundwater (modeled as a distinct pool of water, Figure1). These water sources defined the water volume available for irrigation. WBMplus applied sufficient irrigation water to each grid cell to fulfill the irrigation demand, bringing the soil in the grid cell's irrigated area up to field capacity. This water was first removed from the (renewable) shallow groundwater pool, then from the river discharge and reservoirs. If these water sources were not sufficient to fulfill demand, then mined groundwater was added from a limitless pool to make up the difference. While the shallow groundwater pool was recharged through infiltration, the mined groundwater pool received no recharge. The mined groundwater pool represented groundwater abstractions in excess of recharge. We assumed that all irrigation demand was met, though in practice this may not always be the case.

Delivery of water from an irrigation water source to the irrigated field is inefficient. An efficiency factor, E_{eff} [0.34 for China [*Döll and Siebert,* 2002], was applied to account for these losses. Gross irrigation demand, I_{gross} [mm day^{-1}] was:

$$I_{gross} = \frac{I_{net}}{E_{eff}} \quad (4)$$

Only the efficient portion of irrigation water (i.e., the water equal to irrigation demand) was added to the soil moisture pool. The daily "inefficient" water (I_{gross}–I_{net}) was split three ways and returned to other pools or fluxes in each grid cell: evaporation, groundwater water recharge, and surface runoff. The amount of inefficient water that evaporated, I_{evap}, is:

$$I_{evap} = \begin{cases} PET - AET & \text{if } (I_{gross} - I_{net}) \geq (PET - AET) \\ I_{gross} - I_{net} & \text{if } (I_{gross} - I_{net}) < (PET - AET) \end{cases} \quad (5)$$

If $(I_{gross}–I_{net}) > PET–AET$, then the remaining inefficient water was divided evenly between groundwater recharge and river discharge.

The sources of irrigation water, both the efficient and inefficient portions, were recorded by the model. We assumed that the contribution of each water source to the total irrigation water amount was the same for both the efficient and the inefficient portions.

2.1.2 Large reservoirs

Large reservoirs were represented in the model as river grid cells with large river water storage capacity.. Unlike other river grid cells, the rules for outgoing discharge were governed by reservoir operation rules. The model applied the same set of rules to all reservoirs. If the reservoir storage was below 80% full, then water was released as the log of the reservoir level, and if the reservoir storage was above 80% full, then water was released as the exponent of the reservoir level; release at 80% capacity was equal to annual mean river discharge in that grid cell. Minimum allowed reservoir release was 20% of the 5-year average annual discharge [*Prusevich et al.,* 2013].

2.2 Crop Yield Model

The DeNitrification-DeComposition (DNDC) model, a process-based model of carbon and nitrogen biogeochemistry in agroecosystems, simulated irrigated and rainfed crop yields (kg

C/ha/yr). The model simulates soil temperature and moisture regimes, soil carbon and nitrogen dynamics, crop growth and yield, nitrogen leaching, and emissions of trace gases for both individual crops and multi-cropping systems, and requires as inputs soil properties, daily weather, and crop management details (e.g., crop type and rotation, fertilization, irrigation, tillage, planting and harvest dates) [*Li,* 2007a]. DNDC has been used extensively for studies of both Chinese and global agriculture [e.g., *Zhang et al.,* 2002; *Wang et al*., 2008; *Qiu et al*., 2009; *Li et al*., 2010; *Deng et al*., 2011*; Han et al*., 2014].

Unlike the gridded spatial structure of WBMplus, DNDC modeled crop growth on a county-based (polygon) system. The model was run from 1981 to 2000 to capture 20 years of weather-driven crop yield and irrigation water demand variability for each county in China. NASA's MERRA climate reanalysis product [*Rienecker et al*., 2011] was used for the temperature and precipitation inputs to DNDC, matching each county to the MERRA grid cell closest to the county polygon center. The average county size in China is similar to the size of a MERRA grid cell [~2,500 km2]. Data on crops grown in single- and multiple-crop rotations for each of China's ~2400 counties came from Qiu et al. [2003]. County soil properties used by DNDC (texture, bulk density, pH and carbon content) were from digitization of the Chinese Third National Soil Survey maps [*Shi et al*., 2004; *Tang et al*., 2006]. All crops in all counties were simulated with both full irrigation (no water stress) and no irrigation (rainfed) for all 20 years, to capture weather-driven interannual variability in rainfed and irrigated crop yields. For the simulations presented here, to represent general changes in fertilization across China, we applied a constant increase (~2% yr^{-1}) in crop-specific fertilizer application rates across China from 1981 to 2000, and a step decrease (36%) in manure application rate in 1990 [*NBS,* 2008]. The crop

distribution represented circa 2000 conditions, and simulated crop yields were de-trended with respect to increases in fertilizer and decrease in manure application rates to achieve c.2000 crop yield rates for all 20 years of the simulation, so yield interannual variability resulted from weather effects only. DNDC planting and harvest dates are from Cui et al. [1994], and crop-specific growth parameters are reported in Li [2007b].

2.3 Data

Both WBMplus and DNDC used daily climate drivers of temperature and precipitation from the MERRA NASA reanalysis product, years 1981 - 2000. Soil and non-crop vegetation data were from the UNESCO/FAO soil map of the world [*FAO/UNESCO*, 2003], and the GRanD database of global dams and reservoirs [*Lehner et al*., 2011] was used for the location and storage capacity of ~7000 large reservoirs globally.

The MIRCA2000 gridded crop maps and crop calendars were used to determine crop areas, planting month, and harvest months in WBMplus for each of 26 crop classes, and up to 4 subcrop types [*Portmann et al*., 2010]. Crop class coefficients (*Kc*), rooting depths (*Rd*), and proportional lengths of growing stages were from Siebert and Döll [2010]. Crop calendars (for planting and harvesting dates) were downscaled from monthly to daily values by assuming mid-month planting and harvesting dates.

2.4 Analysis

While the Qiu et al. [2003] and MIRCA2000 crop distributions for China had substantial

overlap, there were enough differences that two data analysis steps were necessary to harmonize the DNDC model output with the WBMplus output and the MIRCA2000 crop maps. First, county-based DNDC yield data were gridded to the resolution of the WBMplus model (0.5 degree) assigning a crop yield value to each grid cell equal to the area-weighted yields of all counties that overlapped with the grid cell. Second, for each grid cell, the individual crop yields were aggregated to produce one average annual irrigated crop yield value and one average rainfed crop yield value, both in units of $kgCha^{-1}yr^{-1}$ (note that multiple crop yields in a single year were aggregated to a single annual average crop yield). All crop production results are therefore based on the composition of irrigated and rainfed crops in DNDC's crop maps, as opposed to MIRCA2000 crop maps. This aggregation allowed for a comparison of land under irrigated versus rainfed cropping.

Both models were run for 20-year periods, 1981 - 2000, to capture impacts of variability in temperature and precipitation on irrigated and rainfed crop yields and irrigation water demand. The crop areas, irrigated areas, and growing season were static, representing year 2000 agriculture [*Portmann et al.,* 2008; *Qiu et al.*, 2003], and all crop yields were de-trended to year-2000 values with respect to time-varying DNDC model inputs (fertilizer and manure). All time series results therefore show variability in water demand and crop yields as a function of climate, and are not meant to be representative of historical trends in crop yields. From 1981 – 2000, the NASA-MERRA climate product reports an average of 640 mm of rainfall per year over agricultural land in China. The driest year for Chinese agriculture was 1992, in which precipitation averaged 596 mm over agricultural land; the wettest year was 1990 with an average of 695 mm of precipitation over agricultural land. The range in inter-annual variation in

individual counties or grid cells was greater than the national aggregate of ~10%.

Surface water and mined groundwater use for irrigation in each grid cell were assumed to be spread among all irrigated crops proportional to demand. Crop yields directly due to the application of mined groundwater were determined for each grid cell by applying the difference between irrigated and rainfed crop yields to the irrigated area supplied by the mined groundwater:

$$Y_{MinedGW_j} = f_{MinedGW_j} \cdot A_{I_j} \cdot (Y_{I_j} - Y_{RF_j}) \quad (6)$$

Where $f_{MinedGWj}$ is mined groundwater as a fraction of total irrigation water demand for grid cell j, $A_{I,j}$ is irrigated area [ha] in grid cell j, and $Y_{I,j}$ and $Y_{RF,j}$ are irrigated and rainfed crop yields [$kgCha^{-1}$ yr^{-1}] in grid cell j. Gridded results were aggregated to 31 provincial totals.

Crop yield per unit area due to mined groundwater is a function of both mined groundwater demand and the difference between irrigated and rainfed crop yields. Both of these variables are climate-dependent, but also vary in different ways based on other factors such as local surface water storage, soil properties, crop composition, and management practices. The combined effects of these variables determine how vulnerable each province's crop production is to groundwater depletion. To capture the combined effects of these two variables, we defined crop groundwater productivity, *CGP* [$kgC\ ha^{-1}\ mm^{-1}$] to describe the yield gains per unit of mined groundwater for each province p, based on province-level data:

$$CGP_p = \frac{Y_{MinedGW_p}}{MinedGW_p} \quad (7)$$

where CGP_p is the crop groundwater productivity for province p [kgC ha^{-1} mm^{-1}], $Y_{minedGWp}$ is the 20-year average crop yield due to mined groundwater in province p [kgC ha^{-1} yr^{-1}], and $MinedGW_p$ is the 20-year average amount of mined groundwater demand in province p [mmyr^{-1}]. *CGP* provides a method for directly comparing provinces' combined reliance on both mined groundwater use and yield impact for crop production to each other.

3. RESULTS

3.1 Irrigation Water Demand and Supply

Over the 20 years simulated by WBMplus, Chinese agriculture required an average of 330 km^3 yr^{-1} irrigation water withdrawals in order to fulfill gross irrigation demands (Table 2). Irrigation water demand standard deviation over the 20-year simulation was 33 km^{3}year^{-1}, or 10% of demand. This deviation is significantly higher than the deviation in annual average rainfall over cropped land, which is only 5% of the mean. Irrigation water demand varies significantly across China, but generally follows patterns of irrigated area (Figure 2).

WBMplus tracks the sources of irrigation water, grouping them into three categories: 1) rivers and reservoirs, 2) renewable groundwater, and 3) mined/fossil groundwater mining (Figure 3). Over the 20-year simulation period, the nationally aggregated amount of irrigation water available from the first two sources are very steady. Rivers and reservoirs supply 115 km^3 yr^{-1}, with a standard deviation of only 7 km^3 yr^{-1} and a range of 105 - 134 km^3 yr^{-1}. Similarly, the average groundwater recharge supplied to irrigation is 107 km^3 yr^{-1}, with a standard deviation of 7 km^3 yr^{-1} and a range of 96 to 125 km^3 yr^{-1}. Due to the extremely steady supply of river and reservoir water as well as groundwater recharge, most of the variability in irrigation water demand leads to widely ranging fossil groundwater mining demands. Average mined groundwater demand is 125 km^3 yr^{-1}, only slightly over one third of the total average irrigation water demand. However, at its maximum demand of 209 km^3 yr^{-1}, mined irrigation water makes up 49% of that year's total irrigation water demand, and at its minimum demand of 58 km^3 yr^{-1} it makes up only 20% of total irrigation water demand.

Demand for mined groundwater varies significantly across China, both in absolute volume and in its relative fraction of total irrigation water demand (Figure 4 and Table 3). These two measures of the importance of mined groundwater do not always vary together. Anhui, the province with the largest irrigated area in MIRCA2000, also has the greatest demand for mined groundwater both in terms of absolute volume (32 km^3 yr^{-1}) and fraction of the province's total irrigation water demand (58%). In contrast, Fujian province has a relatively low mined groundwater demand (3 km^3 yr^{-1}), yet this demand makes up 64% of its total irrigation water demand. Yet a different pattern appears in Shandong province, which has the greatest total irrigation water demand (33 km^3 yr^{-1}), but only 20% of this demand is from mined groundwater.

3.2 Crop Yields

We estimate an average total national crop production of 495 mega-tonnes (Mt)C yr^{-1} (Table 2) if all irrigation requirements are fully met on irrigated cropland (as defined by MIRCA2000 irrigated crop maps). Irrigated land produces 315 Mt C, and rainfed land produces 180 Mt C. Grid-cell crop yields for irrigated and rainfed crops are area-weighted averages across all crops

and rotations occurring in the grid cell (Figure 5). These yields are direct results from the DNDC model, and reflect the spatial variability of crop maps, soil quality, climate, and management practices, in particular single- vs. multi-cropping. The difference in yields follows a general north-south pattern (Figure 5), with the largest differences in the relatively dry north, and the smallest differences in the wetter south.

3.3 Crop Production from Mined Groundwater

When all irrigation water demands are fully met, mined groundwater directly contributes to a large portion of China's national crop production (Figure 6). We estimate an average of 102 Mt C over the 20 year period modeled, with a wide range varying from 79 to 130 Mt C per year due to weather variability (Table 2). The maximum contribution is seen in the driest weather year, and makes up 27% of the total national production; the minimum occurs in the wettest weather year and is 15% of the total national production. Without mined groundwater, the average national crop production is 393 Mt C/year (Figure H), which is 79% of the 20-year average crop production with mined groundwater used as needed.

There are significant regional differences in crop yields produced from irrigation water (Figure 5 & Table 5). Of all the major agricultural provinces, Sichuan has the highest crop irrigation water productivity, gaining 26 kgC/ha/mm (Table 5). There is a decline in crop irrigation water productivity with an increase in precipitation (Figure 7), which indicates that rainfed crop yields in the southern high-precipitation regions of China are close to the maximum yield possible given soil quality, crop selection, and management choices.

We use the crop groundwater productivity, *CGP* (Eq. 7), to compare the vulnerability of provinces to the loss of unsustainably mined groundwater. Xinjiang Province had the maximum 20-year average mined groundwater demand, 596 mm/year, and Tianjin Province had the maximum 20-year average crop yield due to mined groundwater, 3,300 $kgCha^{-1}$. Tianjin also had the highest *CGP*, 11.6 $kgCha^{-1}mm^{-1}$. Beijing and Xinjiang have a *CGP* of 0 kgC ha^{-1} mm^{-1}because simulated use of mined groundwater is zero. Of the major agricultural producers (red in Table 4), Henan, Shandong, and Sichuan have the highest *CGPs* (Figure 8), 7.3, 5.3, and 3.9 kgC ha^{-1} mm^{-1}, respectively. Demand for mined groundwater and crop irrigation water productivity in these provinces were also the most variable based on changes in climate over the 20-years of climate input modeled. The relative importance of mined groundwater versus crop yield gains due to mined groundwater vary between provinces; Sichuan Province has a high *CGP* mainly due to its high mined groundwater demand, while Henan Province has a high *CGP* because of its large crop yield gains due to mined groundwater. However, all provinces fall on a roughly linear trend between low *CGP* and high *CGP* (Figure 8). This trend is not unexpected, as both variables contributing to *CGP* are affected by climate; dry regions have a high demand for mined groundwater and a large crop irrigation water productivity, while wet regions have the opposite (Figure 8).

4. DISCUSSION

4.1 Comparison to other studies

4.1.1 Irrigation water demand and supply

Our results for China's irrigation water demand are similar to other model-based estimates;

previous results range from 220 to 850 km^3 yr^{-1}, with most studies estimating an average of 350 – 400 km^3 yr^{-1} circa 2000. These results assume that gross irrigation water demand was always fulfilled and that the infrastructure is in place to change the source of water depending on the availability. While global irrigation water demand estimates also vary, this study's estimate of 330 km^3 yr^{-1} is roughly 10% - 20% of world-wide demand [*Döll and Siebert,* 2002; *Wisser et al.,* 2008; *Wada et al.,* 2012]. FAO's AQUASTAT database reports China's irrigation water withdrawals to be 358 km^3 yr^{-1}, and Döll and Siebert [2002] report an irrigation water demand of 364 km^3 yr^{-1} for all of East Asia. Wada et al. [2014] use the PCR-GLOBWB model, which is similar in structure to WBMplus, and report China's irrigation water demand to be 519 km^3 yr^{-1} when the model is driven with the MERRA climate product. Previous studies also report that China's groundwater withdrawals for irrigation are ~100 km^3 yr^{-1} (Table 6), however the only study that distinguishes groundwater recharge from groundwater mining estimates a significantly smaller amount of mined groundwater, 17 - 27 km^3 yr^{-1} [*Wada et al.,* 2012], than this study (58 – 209 km^3 yr^{-1}). Wada et al. [2012] also estimate a "nonlocal water resource" demand of 11 km^3 yr^{-1}, a water supply that is represented in this study's mined groundwater accounting. The remainder of the difference is likely due to the use of different methods for estimating renewable groundwater, and for partitioning of inefficient irrigation water, which has the potential to significantly alter the groundwater recharge. Wada et al. [2012] allow inefficient irrigation water to contribute to groundwater recharge, limited only by the hydraulic conductivity of the soils underlying irrigated areas. In this study, inefficient irrigation water first evaporates to fulfill the difference between AET and PET, then any remaining water is divided equally between groundwater recharge and the river network (Eq. 5).

4.1.2 Crop production

This study estimates a similar total crop production as the National Bureau of Statistics of China, which reports year 2000 crop production was 500 Mt C. This estimate is significantly lower than the year-2000 total crop production of 715 Mt C reported by FAO (Table 6). The difference between the FAO's annual production and this study's production is mainly due to differences in rainfed crops, as the irrigated crop production estimates are comparable at 315 MtC (this study) versus 323 Mt C [FAO]. Our results were consistent with other crop productivity studies that show crop production increases by slightly less than two times due to irrigation [*Siebert and Döll*, 2010; *Molden et al.,* 2007], since irrigated and rainfed harvested areas in China are roughly equal [MIRCA2000; Table 2].

In a study by Ye et al [2013], the CERES crop models (one for each crop simulated) are used to estimate baseline (years 1961 – 1990) crop production in China, as well as future (2030 – 2050) crop production under various climate change scenarios. Baseline crop yields match well with this study at 532 MtC, while future estimates show increasing yields but make no considerations of future water use or availability. Siebert and Döll [2010] use a gridded hydrology model that is similar in structure to WBMplus, and input the MERRA climate product to simulate global crop water demand. They then use an empirical method that relates the simulated AET/PET ratio to the relative ratio between irrigated and rainfed crop yields to calculate crop production due to consumptive irrigation water [*Siebert and Döll*, 2010]. While they do not report values for China, their results show that total crop production across all of East Asia is 545 MtC, and 78.2% (or 457 Mt) is from irrigated agriculture.

462 4.2 Groundwater depletion and crop production

463 In an analysis with multiple global climate models, gridded crop models, and hydrological
464 models of renewable surface water resources, Elliot et al. [2014] simulated future crop
465 production (up to 2090) and found significant decreases due to a combination of climate change
466 and reduced water supply. However, Elliot et al. [2014] included only surface water supplies in
467 their analysis. We explicitly separated the fossil mined groundwater irrigation from renewable
468 groundwater irrigation and surface water irrigation so that we can estimate irrigation water
469 coming from a non-renewable source. Therefore, our estimates of crop yields due to irrigation
470 from mined groundwater show that without this water source, China's total annual crop
471 production would decrease by 15% - 27%, bringing it down to 352 – 448 MtC (Table 2). Annual
472 grain production in China was ~ 350 MtC in the early 1980s, and ~450 MtC in the early to mid
473 1990s [*NBS,* 2008]. Our results assume that groundwater mining occurred at the level necessary
474 to fulfill irrigation water demand after renewable water sources were used. While it is likely that
475 not all irrigated areas are always provided with 100% of their irrigation water demand, there is
476 abundant evidence, both observational and modeling studies, that groundwater depletion is
477 occurring in China, particularly in the North China Plain [*Wada et al.,* 2012b; Aeschbach-Hertig
478 and Gleeson, 2012; Syed et al., 2008; Tang et al., 2013]. Results from the Gravity Recovery and
479 Climate Experiment (GRACE) satellite show contemporary groundwater depletion rates of 8.4 –
480 14 mm yr^{-1} in the North China Plain, and further analysis by Tang et al [2013] shows these rates
481 may underestimate depletion by ~7.6 mm yr^{-1}.
482
483 The North China Plain includes much of Henan, Hebei, Shandong, northern Jiangsu, and
484 northern Anhui provinces, all of which are significant agricultural producers (Table 4). These

485 five provinces collectively produce 152 Mt Cyr^{-1} (31% of total national production). Anhui and
486 Jiangsu rely on mined groundwater for 42% and 49% of their total irrigation water supplies, and
487 Henan, Hebei, and Shandong rely even more heavily on mined groundwater, requiring on
488 average 73%, 77%, and 80% of their annual irrigation water to come from groundwater mining.
489 Without the use of mined groundwater, crop production in the North China Plain would drop to
490 101 MtC yr^{-1}, a 10% loss in national production.
491
492 Groundwater depletion is also occurring in the northern-most and western-most parts of China
493 [*Aeschbach-Hertig and Gleeson*, 2012; *Syed et al.,* 2008], affecting Heilongjiang, Jilin, Nei
494 Mongol, and Xinjiang Provinces, which are all relatively small agricultural producers (Table 4).
495 Of these smaller agricultural producers, Jilin has the lowest relative reliance on mined
496 groundwater, at 70%, and Xinjiang has the highest at 80%. Northern provinces also have
497 extremely large differences between irrigated and rainfed crop yields (Figure 5), so that even a
498 small loss of irrigation water causes a substantial decrease in their crop production.
499
500 We used the crop groundwater productivity, *CGP* (see Eq.7), to assess which provinces are
501 vulnerable to the loss of unsustainably mined groundwater. Vulnerability can be due to either a
502 high reliance on mined groundwater, significant crop yields dependent upon mined groundwater,
503 or a combination of both these factors. Provinces that have a high *CGP* and are large agricultural
504 producers fall along a band of precipitation with precipitation roughly between 1000 and 1500
505 $mmyr^{-1}$ (Fig.8 inset). South of this band, provinces have low reliance on mined groundwater and
506 small increases to crop yields due to use of mined groundwater. North of this band, provinces
507 have high *CGP*s, but they are not large agricultural producers. Therefore we expect that if
508 groundwater levels continue to drop, the provinces in this precipitation band will have decreased

crop yields unless they can secure alternative water supplies or significantly increase crop water use efficiency [e.g., *Liu et al*., 2010]. China's southern provinces, many of which are significant agricultural producers, are less at risk of aquifer depletion than northern provinces [*Döll et al.,* 2012], and their *CGPs* are low.

4.3 Limitations and uncertainties

Uncertainties, sensitivity analysis, and model validation for WBMplus are discussed in Wisser et al [2010], and for DNDC in Li et al [1992a], Li et al [1994], and Wang et al [2008]. Additional uncertainty introduced in this study arises from combining the two models' results, which are based on different crop maps. While the national total irrigated and rainfed areas are similar, MIRCA2000 (WBMplus input) and DNDC's crop maps disagree on which type of crops are grown on 63% of irrigated areas, and 31% of rainfed areas. DNDC also represents crop rotations at a more detailed level than MIRCA2000 [*Qiu et al.,* 2003]. This uncertainty does not significantly impact the results of this study because both sets of model results have been validated or tested against other studies, and are both predicting results consistent with observational data and other modeling studies. Our conclusions and interpretations only address the total water demand and crop production of all irrigated and rainfed crops, and we do not make any interpretations about individual crop types; this type of analyses would require crop maps with better agreement.

Paddy rice is a major consumer of irrigation water and so representation of paddy water management and water balance has significant impact on WBMplus results for China. There was a significant change in rice paddy water management in China during 1980-2000, with most

farmers adopting a mid-season draining or drying management scheme [*Li et al*., 2002]. This practice was adopted to save labor and energy, and may also conserve water (we are not aware of any studies that have quantified water savings impacts). Paddy mid-season draining/drying has not been implemented in WBMplus, so paddy irrigation water use may be overestimated in our analysis.This over-estimation may be offset by an under-estimation of the water amounts required to initially flood rice paddies. WBMplus's rice paddy flooding implementation applies 50mm of water above soil field capacity, which would be insufficient to inundate many field soils. Finally, macro-scale modeling that relates flooded paddy percolation losses to soil texture may overestimate losses in paddies that have been in managed use for centuries (e.g., the Sichuan Basin), where paddy percolation losses may be lower than would estimated from regional soil properties.

5. Conclusions

This study is the first to combine a hydrologic model with a process-based crop growth model to simulate national-scale agricultural yield and irrigation water use. This methodology allows for the direct attribution of crop yields to irrigation water from rivers and reservoirs, groundwater, and fossil mined groundwater (Figure 2), as well as computation of the spatially varying crop water productivity from total irrigation water, and the crop groundwater productivity. We find that mined groundwater fulfills 20% - 49% of China's national irrigation water demand, which directly leads to 15% - 27% of national crop production. Crop water productivity and mined groundwater demand vary spatially across China, with the combination leading to a smaller percentage of crop yields dependent upon mined groundwater than the percent of total irrigation water demand fulfilled by mined groundwater. I.e., while mined groundwater fulfills 20% - 49%

of irrigation water demand, crops irrigated with mined groundwater only account for 15% - 27% of national crop production, which indicates that the regions with high crop yields are not all directly dependent upon mined groundwater. This study calculated a crop groundwater productivity to determine which provinces would be most vulnerable to the loss of access to mined groundwater. We found that provinces across central China are most vulnerable due to their combination of significant agricultural production, high demand for mined groundwater, and high crop yield gains from the use of mined groundwater.

China, like all major world agricultural producers, has increased irrigation to the point of over-exploitation of water resources in order to achieve greater levels of food production. While irrigation is typically employed to reduce agriculture's vulnerability to weather and climate variability, in the case of water over-exploitation irrigated agriculture may be vulnerable to changes in the water supply caused by both climate variability and diminishing water resources. We find that these two factors – climate variability and mined groundwater demand – do not operate independently, but rather magnify one another by increasing the demand for irrigation water in a hot and dry year while simultaneously reducing the water available for irrigation use. Due to this magnification, the amount of food production dependent upon irrigation from unsustainable water supplies varies significantly from year to year.

Understanding the sources of irrigation water supply and their relative importance to crop production across China will help provide context for water resource management in China, especially with regards to groundwater storage and the South-North Water Transfer Project. Global depletion of groundwater aquifers, including the North China Plain, will require future

groundwater use to achieve greater levels of sustainability than are seen today. Simultaneously, crop production will need to increase to feed the growing world population. Increases in crop water productivity are required to achieve these two goals. A major finding of this research is that crop irrigation water productivity varies significantly across China and that inter annual weather variability results in widely ranging responses in crop irrigation water productivity, as well as in relative reliance on mined groundwater. The wide range in crop water productivity can help identify the regions in China where climate, soil conditions, and management practices work together to achieve high levels of "crop per drop". Increasing cropping efficiency will likely be a key component of feeding the world's growing population in a sustainable manner [*Brauman et al*., 2013]. Similarly, the distinction between crop yield losses due primarily to yield differences versus reliance on mined groundwater illustrates that different strategies (e.g., increasing rainfed yields versus reducing reliance on mined groundwater) will be best suited to different regions in order to achieve the future requisite increases in crop productivity within the constraints of future water availability.

Acknowledgments – This work was supported by NSF Water, Sustainability, and Climate Program (grantEAR-1038818), and the National Science Foundation Graduate Research Fellowship Program under Grant No. DGE-0913620.
This work was also supported by the U.S. Department of Energy, Office of Science, Biological and Environmental Research Program, Integrated Assessment Program, Grant No. DE-SC0005171.

603 REFERENCES

604 Aeschbach-Hertig, W. and T. Gleeson (2012), Regional strategies for the accelerating global
605 problem of groundwater depletion, *Nature Geoscience, 5*(12), 853-861, doi:
606 10.1038/NGEO1617.

607 Allen, R. G. (1998), Crop Evapotranspiration: Guidelines for Computing Crop Water
608 Requirements, *FAO Irrigation and Drainage Paper, 56*.

609 AQUASTAT , FAOs global information system of water and agriculture, *2008*.

610 Cai, X., D. Molden, M. Mainuddin, B. Sharma, A. Movin-ud-Din, and P. Karimi (2011),
611 Producing more food with less water in a changing world: assessment of water productivity in 10
612 major river basins, *Water International, 36*, 42-62.

613 Calow, R. C., S. E. Howarth, and J. Wang (2009), Irrigation Development and Water Rights
614 Reform in China, *Int. J. Water Resour. Dev., 25*(2), doi: 10.1080/07900620902868653.

615 Cui, D., H. Liu, J. Min, and J. He (1994), *Atlas of Phenology for Major Crops in China*,
616 Meteorological Press, Beijing.

617 Deng, J., Z. Zhou, B. Zhu, X. Zheng, C. Li, X. Wang, and Z. Jian (2011), Modeling nitrogen
618 loading in a small watershed in southwest China using a DNDC model with hydrological
619 enhancements, *Biogeosciences, 8*(10), 2999-3009, doi: 10.5194/bg-8-2999-2011.

620 Doell, P., H. Hoffmann-Dobrev, F. T. Portmann, S. Siebert, A. Eicker, M. Rodell, G. Strassberg,
621 and B. R. Scanlon (2012), Impact of water withdrawals from groundwater and surface water on
622 continental water storage variations, *Journal of Geodynamics, 59*, 143-156, doi:
623 10.1016/j.jog.2011.05.001.

624 Doll, P. and S. Siebert (2002), Global modeling of irrigation water requirements, *Water Resour.*
625 *Res., 38*(4), 1037, doi: 10.1029/2001WR000355.

626 Elliott, J. et al. (2014), Constraints and potentials of future irrigation water availability on
627 agricultural production under climate change, *Proc. Natl. Acad. Sci. U. S. A., 111*(9), 3239-3244,
628 doi: 10.1073/pnas.1222474110.

629 Federer, C. A., C. Vorosmarty, and B. Fekete (1996), Intercomparison of methods for calculating
630 potential evaporation in regional and global water balance models, *Water Resour. Res., 32*(7),
631 doi: 10.1029/96WR00801.

632 Foley, J. A. et al. (2011), Solutions for a cultivated planet, *Nature, 478*(7369), doi:
633 10.1038/nature10452.

634 Hamon, W. R. (1963), Computation of direct runoff amounts from storm rainfall, *International*
635 *Association of Sciences Hydrology Publications, 63*, 52-62.

636 Han, J., Z. Jia, W. Wu, C. Li, Q. Han, and J. Zhang (2014), Modeling impacts of film mulching
637 on rainfed crop yield in Northern China with DNDC, *Field Crops Res., 155*, 202-212, doi:
638 10.1016/j.fcr.2013.09.004.

639 Kang, Y., S. Khan, and X. Ma (2009), Climate change impacts on crop yield, crop water
640 productivity and food security - A review, *Progress in Natural Science, 19*(12), doi:
641 10.1016/j.pnsc.2009.08.001.

642 Lehner, B. et al. (2011), High-resolution mapping of the world's reservoirs and dams for
643 sustainable river-flow management, *Frontiers in Ecology and the Environment, 9*(9), 494-502,
644 doi: 10.1890/100125.

645 Li, C. S., S. Frolking, and T. A. Frolking (1992), A Model of Nitrous-Oxide Evolution from Soil
646 Driven by Rainfall Events .1. Model Structure and Sensitivity, *Journal of Geophysical Research-*
647 *Atmospheres, 97*(D9), 9759-9776.

648 Li, C. S., S. Frolking, and T. A. Frolking (1992), A Model of Nitrous-Oxide Evolution from Soil
649 Driven by Rainfall Events .2. Model Applications, *Journal of Geophysical Research-*
650 *Atmospheres, 97*(D9), 9777-9783.

651 Li, C. S., S. Frolking, and R. Harriss (1994), Modeling Carbon Biogeochemistry in Agricultural
652 Soils, *Global Biogeochem. Cycles, 8*(3), 237-254, doi: 10.1029/94GB00767.

653 Li, C. S., J. J. Qiu, S. Frolking, X. M. Xiao, W. Salas, B. Moore, S. Boles, Y. Huang, and R. Sass
654 (2002), Reduced methane emissions from large-scale changes in water management of China's
655 rice paddies during 1980-2000, *Geophys. Res. Lett., 29*(20), 1972, doi: 10.1029/2002GL015370.

656 Liu, Q. and Z. Yang (2010), Quantitative estimation of the impact of climate change on actual
657 evapotranspiration in the Yellow River Basin, China, *Journal of Hydrology, 395*(3-4), 226-234,
658 doi: 10.1016/j.jhydrol.2010.10.031.

659 Liu, Y., S. Li, F. Chen, S. Yang, and X. Chen (2010), Soil water dynamics and water use
660 efficiency in spring maize (Zea mays L.) fields subjected to different water management
661 practices on the Loess Plateau, China, *Agric. Water Manage., 97*(5), 769-775, doi:
662 10.1016/j.agwat.2010.01.010.

663 Li, C. (2007), Quantifying greenhouse gas emissions from soils: Scientific basis and modeling
664 approach, *Soil Sci. Plant Nutr., 53*(4), 344-352, doi: 10.1111/j.1747-0765.2007.00133.x.

665 Ma, J., A. Y. Hoekstra, H. Wang, A. K. Chapagain, and D. Wang (2006), Virtual versus real
666 water transfers within China, *Philosophical Transactions of the Royal Society B-Biological*
667 *Sciences, 361*(1469), 835-842, doi: 10.1098/rstb.2005.1644.

668 Molden, D. and T. Y. Oweis (2007), Pathways for increasing agricultural productivity, in *Water*
669 *for Food, Water for Life: A Comprehensive Assessment of Water Management in Agriculture*,
670 edited by D. Molden, pp. 279-310, IMWI, Earthscan, London.

Mueller, C. and R. D. Robertson (2014), Projecting future crop productivity for global economic modeling, *Agricultural Economics, 45*(1), 37-50, doi: 10.1111/agec.12088.

NBS (National Bureau of Statistics of China) (2008), *China Statistical Yearbook*, National Bureau of Statistics of Chin, Beijing.

Portmann, F. T., S. Siebert, and P. Doell (2010), MIRCA2000-Global monthly irrigated and rainfed crop areas around the year 2000: A new high-resolution data set for agricultural and hydrological modeling, *Global Biogeochem. Cycles, 24*, GB1011, doi: 10.1029/2008GB003435.

Prusevich, A. A., A. I. Shiklomanov, S. Frolking, S. Glidden, R. B. Lammers, and D. Wisser (2013), Log-Exponential Reservoir Operating Rules for Global And Regional Hydrological Modeling, *Eos Transactions, AGU, Fall Meeting Supplement, abstrct GC21B-0827, 94*.

Qiu, J., T. Huajun, S. Frolking, S. Boles, C. Li, X. Xiangming, J. Liu, Y. Zhuang, and X. Qin (2003), Mapping Singe-, Double-, and Triple-crop Agriculture in China at 0.5^{o} x 0.5^{o} by Combining County-scale and Census Data with a Remote Sensing-derived Land Cover Map, *Geocarto Internationa, 18*.

Qiu, J., C. Li, L. Wang, H. Tang, H. Li, and E. Van Ranst (2009), Modeling impacts of carbon sequestration on net greenhouse gas emissions from agricultural soils in China, *Global Biogeochem. Cycles, 23*, GB1007, doi: 10.1029/2008GB003180.

Rienecker, M. M. et al. (2011), MERRA: NASA's Modern-Era Retrospective Analysis for Research and Applications, *J. Clim., 24*(14), 3624-3648, doi: 10.1175/JCLI-D-11-00015.1.

Shi, X., D. Yu, E. D. Warner, X. Pan, G. W. Petersen, Z. G. Gong, and D. C. Weindorf (2004), Soil database of 1:1,000,000 digital soil survey and reference system of the Chinese genetic soil classification system, *Soil Survey Horizons, 45*, 129-136.

Shiklomanov, I. A. and J. C. Rodda (Eds.) (2003), *World Water Resources at the Beginning of the 21st Century, UNESCO International Hydrology Press Ed.*, Cambridge University Press.

Siebert, S. and P. Doell (2010), Quantifying blue and green virtual water contents in global crop production as well as potential production losses without irrigation, *Journal of Hydrology, 384*(3-4), doi: 10.1016/j.jhydro1.2009.07.031.

Syed, T. H., J. S. Famiglietti, M. Rodell, J. Chen, and C. R. Wilson (2008), Analysis of terrestrial water storage changes from GRACE and GLDAS, *Water Resour. Res., 44*(2), W02433, doi: 10.1029/2006WR005779.

Tang, H., J. Qiu, E. Van Ranst, and C. Li (2006), Estimations of soil organic carbon storage in cropland of China based on DNDC model, *Geoderma, 134*(1-2), 200-206, doi: 10.1016/j.geoderma.2005.10.005.

Tang, Q., X. Zhang, and Y. Tang (2013), Anthropogenic impacts on mass change in North China, *Geophys. Res. Lett., 40*(15), 3924-3928, doi: 10.1002/grl.50790.

Tilman, D., K. G. Cassman, P. A. Matson, R. Naylor, and S. Polasky (2002), Agricultural sustainability and intensive production practices, *Nature, 418*(6898), 671-677, doi: 10.1038/nature01014.

Vorosmarty, C. J., C. A. Federer, and A. L. Schloss (1998), Evaporation functions compared on US watersheds: Possible implications for global-scale water balance and terrestrial ecosystem modeling, *Journal of Hydrology, 207*(3-4), doi: 10.1016/S0022-1694(98)00109-7.

Vorosmarty, C. J., B. M. Fekete, M. Meybeck, and R. B. Lammers (2000), Geomorphometric attributes of the global system of rivers at 30-minute spatial resolution, *Journal of Hydrology, 237*(1-2), 17-39, doi: 10.1016/S0022-1694(00)00282-1.

Wada, Y., D. Wisser, and M. F. P. Bierkens (2014), Global modeling of withdrawal, allocation and consumptive use of surface water and groundwater resources, *Earth System Dynamics, 5*, 15-40.

Wada, Y., L. P. H. van Beek, and M. F. P. Bierkens (2012), Nonsustainable groundwater sustaining irrigation: A global assessment, *Water Resour. Res., 48*, W00L06, doi: 10.1029/2011WR010562.

Wang, L., J. Qiu, H. Tang, H. Li, C. Li, and E. Van Ranst (2008), Modelling soil organic carbon dynamics in the major agricultural regions of China, *Geoderma, 147*(1-2), 47-55, doi: 10.1016/j.geoderma.2008.07.009.

Wisser, D., B. M. Fekete, C. J. Voeroesmarty, and A. H. Schumann (2010), Reconstructing 20th century global hydrography: a contribution to the Global Terrestrial Network- Hydrology (GTN-H), *Hydrology and Earth System Sciences, 14*(1), 1-24.

Wisser, D., S. Frolking, E. M. Douglas, B. M. Fekete, C. J. Voeroesmarty, and A. H. Schumann (2008), Global irrigation water demand: Variability and uncertainties arising from agricultural and climate data sets, *Geophys. Res. Lett., 35*(24), L24408, doi: 10.1029/2008GL035296.

Ye, L. et al. (2013), Climate change impact on China food security in 2050, *Agronomy for Sustainable Development, 33*(2), 363-374, doi: 10.1007/s13593-012-0102-0.

Zhang, Y., C. S. Li, C. C. Trettin, H. Li, and G. Sun (2002), An integrated model of soil, hydrology, and vegetation for carbon dynamics in wetland ecosystems, *Global Biogeochem. Cycles, 16*(4), 1061, doi: 10.1029/2001GB001838.

TABLES

Table 1: Data sets input to WBM and DNDC.

Data Type	**Variables**	**WBM Source**	**DNDC Source**
Climate Drivers	Temperature Precipitation	MERRA	MERRA, (Reinecker et al. 2011)
Soil Properties	Field Capacity Wilting Point Non-crop rooting depth Soil drainage class	FAO Soil Map of the World	Third National Soil Survey (Shi et al. 2004)
Crop Distribution	Irrigated crops and areas Rainfed crops and areas	MIRCA 2000	Qiu et al. 2003
Crop Calendar	Plant Date Harvest Date	MIRCA 2000	Cui et al 1984
Crop water use parameters	Rooting Depth Crop Coefficient Growth Stages	Siebert and Doll (2010)	Li 2007b

Table 2: China national 20-year mean and range of irrigated and rainfed areas, annual irrigation water demand, crop yields, and the difference between sustainable and unsustainable yields.

Variable	**Mean**	**Range**
Irrigated area (ha)	79,100,000	
Rainfed area (ha)	76,600,000	
Irrigation water demand (km3/yr)	330	270 - 420
Mined groundwater demand (km3/yr)	125	58 - 209
Fully irrigated yield (MMTC/yr)	315	308 - 321
Rainfed yield (MMTC/yr)	180	164 - 207
Sum: Irrigated + Rainfed yields	495	474 - 527
Sustainable irrigated yield (MMTC/yr)	127	114 - 142
Sustainable rainfed yield (MMTC/yr)	265	238 - 305
Sum: Irrigated + Rainfed yields	393	352 - 448
Unsustainable minus Sustainable Yields (Mt C/yr)	102 (21%)	79 – 130 (15% - 27%)

Table 3: Province summary of irrigation water demand, and mined groundwater demand.

Province	Harvested Irrigated Area (Mha)	Irrigation Demand (km^3/yr)	Mined Groundwater Demand (km^3/yr)	Mined Groundwater Demand (fraction total)
Anhui	6.8	32	13	0.42
Jiangsu	5.2	26	13	0.49
Hunan	4.9	19	6	0.33
Jiangxi	3.6	16	5	0.33
Zhejiang	2.7	12	4	0.35
Hubei	3.4	13	5	0.39
Shandong	6.6	33	26	0.80
Henan	7.1	25	28	0.73
Guangdong	2.2	8	3	0.33
Guangxi	2.5	8	3	0.33
Hebei	4.6	24	18	0.77
Fujian	1.3	5	2	0.33
Guizhou	1.3	5	2	0.33
Yunnan	2.2	5	2	0.33
Sichuan	2.6	15	10	0.69
Chongqing	1.0	6	4	0.65
Jilin	2.2	6	4	0.70
Liaoning	2.2	6	4	0.69
Xinjiang Uygur	3.9	29	23	0.80
Heilongjiang	2.5	6	4	0.70
Shaanxi	2.1	7	5	0.75
Hainan	0.18	1	0.3	0.33
Shanghai	0.14	1	0.4	0.43
Shanxi	1.45	3	2	0.83
Nei Mongol	3.3	13	10	0.81
Tianjin	0.54	2	2	0.77
Gansu	1.3	4	3	0.80
Ningxia Hui	0.51	3	2	0.82
Qinghai	0.49	1	0.8	0.75
Beijing	0.15	0	0	
Xizang	0.16	0	0	

Table 4: China province 20-year average sustainable and unsustainable crop yields, with 20-year minimum and maximum yields in parentheses.

	Province	Total Crop Yield [Mt C]	Crop Yield without mined groundwater [Mt C]	Cumulative percent of national total crop yield	Cumulative percent of national total crop yield without mined groundwater
	Hunan	**39** (37, 41)	**38** (36, 40)	8	8
	Henan	**37** (33, 42)	**23** (14, 34)	16	13
	Anhui	**36** (33, 39)	**31** (23, 37)	24	20
	Shandong	**29** (25, 32)	**14** (5, 25)	30	23
	Jiangsu	**28** (27, 30)	**24** (19, 31)	36	28
	Jiangxi	**27** (26, 29)	**27** (25, 29)	42	33
	Sichuan	**26** (23, 28)	**22** (19, 25)	47	38
	Guangdong	**25** (24, 26)	**25** (24, 26)	53	43
	Guangxi	**24** (23, 25)	**23** (22, 24)	58	48
	Hubei	**23** (21, 26)	**21** (17, 24)	63	53
	Guizhou	**22** (20, 23)	**21** (20, 22)	67	57
	Hebei	**22** (20, 24)	**9** (3, 16)	72	59
	Zhejiang	**16** (16, 17)	**16** (15, 17)	75	63
	Chongqing	**15** (13, 17)	**13** (10, 15)	79	65
	Yunnan	**14** (14, 15)	**13** (13, 14)	81	68
	Fujian	**14** (12, 14)	**13** (12, 14)	84	71
	Shaanxi	**13** (10, 13)	**7** (4, 10)	87	72
	Jilin	**10** (8, 12)	**7** (5, 10)	89	74
	Liaoning	**9** (7, 10)	**6** (5, 8)	91	75
	Nei Mongol	**9** (9, 10)	**2** (1, 4)	93	76
	Xingjiang	**9** (8,9)	**2** (2, 4)	95	75
	Heilongjiang	**7** (6, 9)	**5** (4, 7)	96	77
	Shanxi	**5** (4, 6)	**3** (1, 4)	97	77
	Gansu	**4** (4, 5)	**1** (1, 3)	98	77
	Tianjin	**3** (3, 3)	**1** (0, 2)	99	78
	Ningxia Hui	**2** (2, 2)	**0** (0, 1)	99	78
	Beijing	**1** (0, 1)	**0** (0, 0)	99	78
	Hainan	**1** (1, 2)	**1** (1, 2)	100	78
	Quinghai	**1** (1, 1)	**0** (0, 1)	100	78
	Shanghai	**1** (1, 1)	**1** (0, 1)	100	78
	Xizang	**0** (0, 0)	**0** (0, 0)	100	78

[a]Provinces are ordered from largest to smallest average annual yields. Color coding on the left indicates: red = top 50% of cumulative national yields; blue = top 75% of cumulative yields; yellow = top 95% of cumulative yields. See Figure S01.

Table 5: Crop yield gains per mm of irrigation water for each of the provinces that contribute to the top 50% of cumulative national yields.

Province	Irrigation Water (mm/yr)	Irr Yield – RF Yield (kgC/ha)	Yield Gain per mm Irrigation Water (kgC/ha/mm)
Sichuan	31	810	26
Henan	135	2164	16
Shandong	253	1854	7
Anhui	219	1416	6
Hunan	92	535	6
Jiangsu	267	1413	5
Guangdong	49	182	4
Jiangxi	93	279	3

Table 6: Estimates of irrigation water use, groundwater abstraction, and crop production from this study and others.

China Irrigation Water Demand (km^3)	**Groundwater Abstraction (km^3)**	**Year**	**Source**
270 – 420	58 – 209	2000	This study
403	97 (20 mined)	2000	Wada et al. 2012
537	95	2000	Wada et al. 2014
358	101	2005	FAO AQUASTAT
220 – 850	*-nr-*	2000	Wisser et al. 2008
358	*-nr-*	2005	Jiang 2009
364*	*-nr-*	1995	Doll and Siebert 2002
China annual crop production (Mt C)	**China irrigated annual crop production (Mt C)**	**Year**	**Source**
474 – 527	315	2000	This study
500	*-nr-*	2000	China Statistical Yearbook
532	*-nr-*	1961 - 1990	Ye et al. 2012
715	323	2000	FAO AQUASTAT
545*	457*	1998 - 2002	Siebert and Doll 2010
474**	*-nr-*	2009	Fan et al. 2012

-nr- results not reported.
*Estimates for all of East Asia
**Cereal production only

Figure Captions

Figure 1: Water stocks and flows in one grid cell of the Water Balance Model (WBM). Irrigation water flows are shown in orange, and inefficient irrigation water returns are shown in gray. Each grid cell can have up to 26 irrigated and rainfed crop types, each with unique root depths. The arrows into and out of the river &reservoir water stock represent water flowing into and out of the grid cell by way of the Simulated Topological River Network.

Figure 2: a) Irrigation area (ha) in each 0.5° grid cell from MIRCA2000, and b) simulated average irrigation water demand (I_{gross} in Eq. 4, mm yr^{-1}).

Figure 3: (top) Annual precipitation ($mmyr^{-1}$) over all cropped areas in China from 1981 – 2000. (middle) Annual national crop yield (Mt Cyr^{-1}) under fully irrigated conditions (purple) and under surface-water-use-only conditions, i.e., without mined groundwater (green). (bottom) China's annual irrigation water demand for 1981 – 2000 (interannual variation from weather variability, not changes in crop or irrigation areas). Irrigation demand is partitioned into supply from rivers and reservoirs (blue), shallow groundwater recharge (orange), and the mined groundwater (black hashed) required to fulfill all irrigated crop demands. Note that plotted yields are based on c.2000 cropping area and management, and only represent interannual variability in weather. Actual grain yields in China increased by about 2.5% - 3% per year during most of 1980 to 2000, due to improved management.

Figure 4: Mean annual mined groundwater required to meet total grid cell irrigation demand (a) in mm, and (b) as fraction of total irrigation demand.

Figure 5: DNDC-simulated grid-cell mean (a) irrigated crop yield, (b) rainfed crop yield, and(c) difference between irrigated and rainfed yields (all $kgCha^{-1}yr^{-1}$). Averages are area-weighted across all crops under irrigation (a) or rainfed (b) systems, and for multiple-cropping, yields are the area-weighted total annual yield per hectare. Where the difference is negative, rainfed yields are higher than irrigated yields because different crops are grown under rainfed and irrigated conditions; in these areas the rainfed crops produce higher yields than the irrigated crops.

Figure 6: Mean annual grid-cell crop yield ($kgCyr^{-1}$) attributed to mined groundwater irrigation.

Figure 7: (a) For each province, a line connects the rainfed crop yield (lower dot on the y-axis), the river, reservoir, and shallow groundwater irrigated crop yield (middle dot), and the fully irrigated crop yield (high dot on the y-axis); all yields in $kgCha^{-1}yr^{-1}$. For the rainfed yields, the water axis (x-axis) is mean annual precipitation over the cropped area in each province. For the irrigated yields, the water axis is the mean annual precipitation [$mmyr^{-1}$] over all cropped area, plus the mean annual irrigation water [$mmyr^{-1}$] applied to irrigated areas. The colors of the lines follow the color scheme for cumulative yields in Table 4, with the black dots and dashed black lines representing the white color-coded provinces from Table 4. Note that the linear relationship between rainfed, surface-water irrigated, and fully-irrigated yields illustrates the assumptions made by integrating the results from WBM and DNDC; these relationships may in reality be non-linear. (b) The slope of lines in part (a) [$kgCha^{-1}$ mm^{-1}] versus annual precipitation over cropland in each province. The slope of the lines in (a) represent the crop yield gain due to irrigation water.

Figure 8: (top) Provinces with high crop groundwater productivity (*CPG*) and high annual crop yields fall in a band of moderate annual precipitation (inset). Each province's crop groundwater productivity (*CPG*) is indicated by the size of the filled circles, and their cumulative yield is indicated by the gray shading. (bottom) *CPG* is a function of both mined groundwater demand and crop yields due to mined groundwater; all provinces fall along a general linear trend when their crop yield gain due to mined groundwater is plotted against mined groundwater demand. Size of symbols proportional to total provincial crop yield, and coloring follows cumulative yield scheme in Table 4.

Figure S01: China provinces. Color indicates the cumulative crop yield categories shown in Table 4: red = top 50% of cumulative national yields; blue = top 75% of cumulative yields; yellow = top 95% of cumulative yields

Figure 1

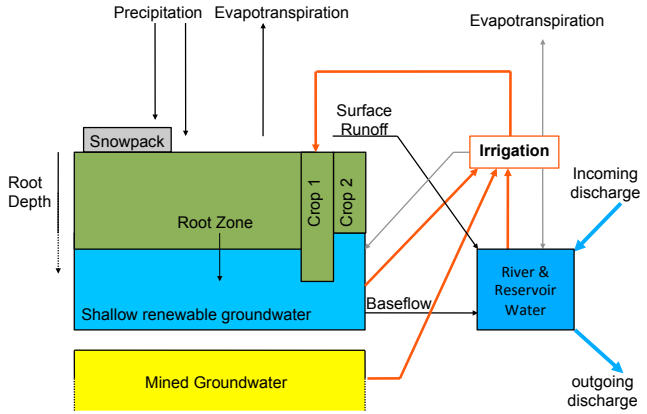

Figure 2

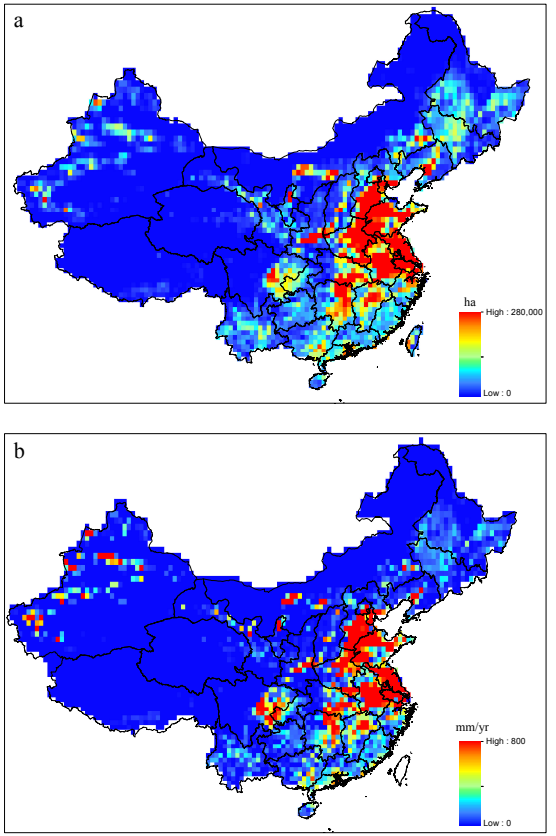

Figure 3

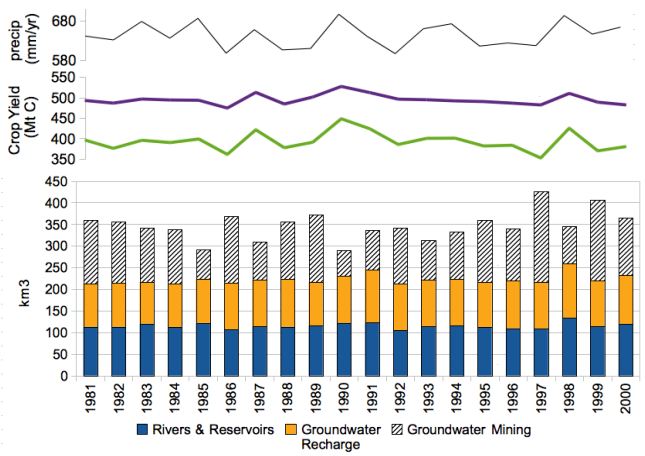

Figure 4

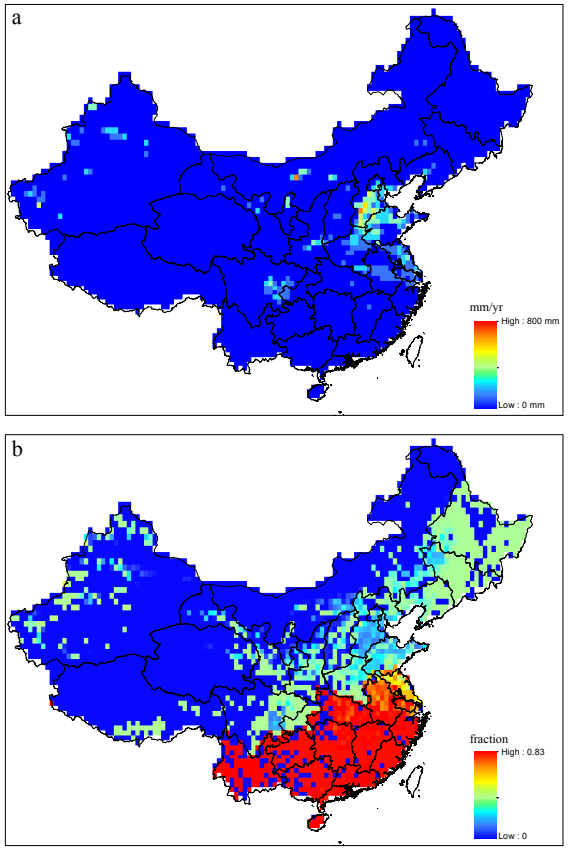

Figure 5

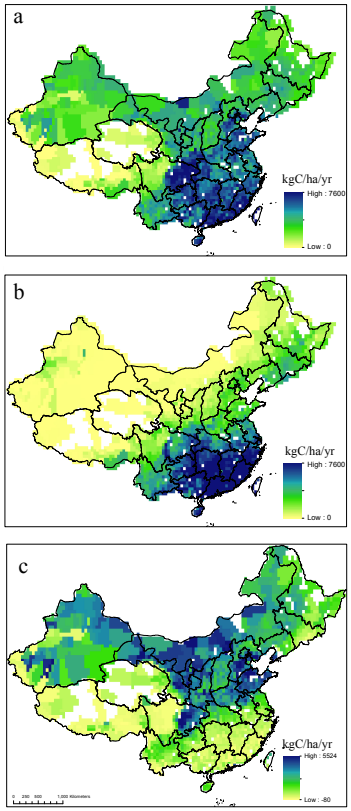

Figure 6

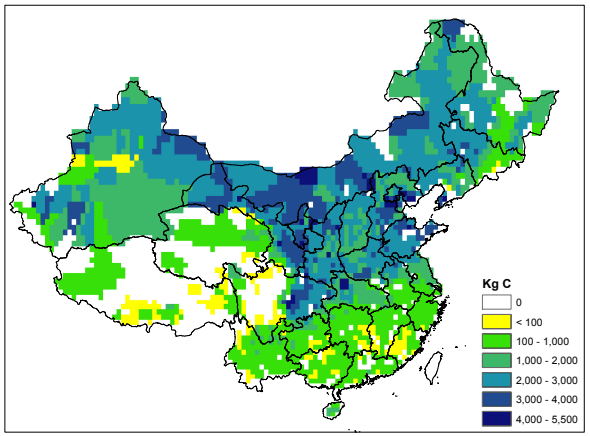

Figure 7

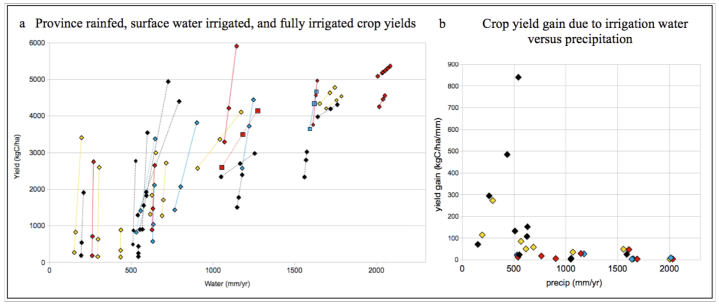

Figure 8

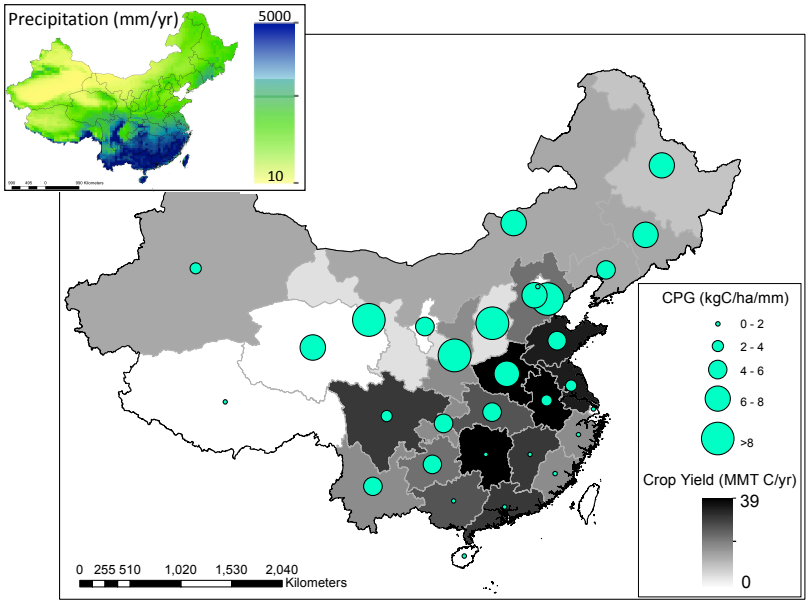

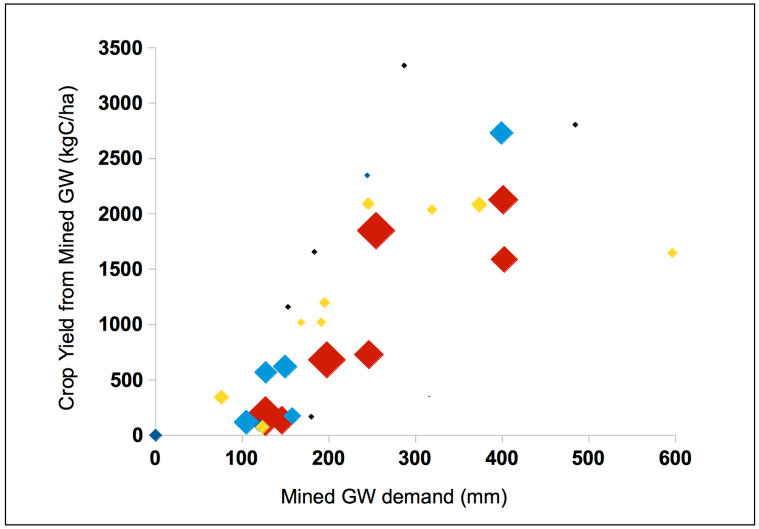

Figure S01

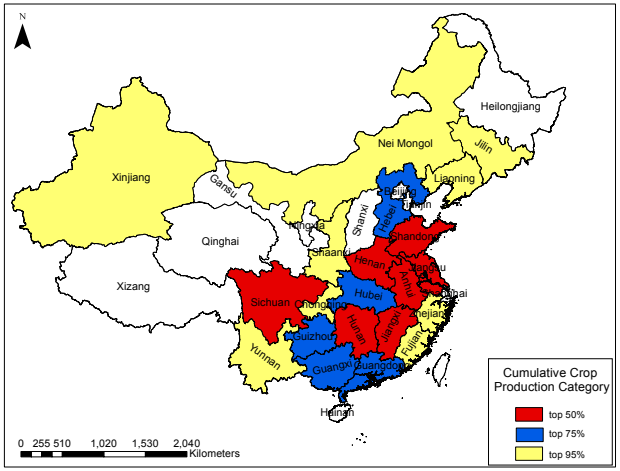
N
Heilongjiang
Nei Mongol
Jilin
Xinjiang
Liaoning
Gansu
Beijing
Tianjin
Hebei
Shanxi
Ningxia
Shandong
Qinghai
Shaanxi
Henan
Jiangsu
Anhui
Shanghai
Xizang
Hubei
Sichuan
Chongqing
Zhejiang
Hunan
Jiangxi
Guizhou
Fujian
Yunnan
Guangxi
Guangdong
Hainan
0 255 510 1,020 1,530 2,040
Kilometers
Cumulative Crop Production Category
top 50%
top 75%
top 95%